Mechanistic Investigations of 1-Aminocyclopropane 1-Carboxylic Acid Oxidase with Alternate Cyclic and Acyclic Substrates †

4 AUTHORS, INCLUDING:

Liviu M Mirica

Washington University in St. Louis

44 PUBLICATIONS **1,967** CITATIONS

SEE PROFILE

Kevin P Mccusker

Edison Pharmaceuticals

8 PUBLICATIONS **98** CITATIONS

SEE PROFILE

Judith P Klinman

University of California, Berkeley

278 PUBLICATIONS **13,064** CITATIONS

SEE PROFILE

Mechanistic Investigations of 1-Aminocyclopropane 1-Carboxylic Acid Oxidase with Alternate Cyclic and Acyclic Substrates[†]

Julia Thrower, Liviu M. Mirica, Kevin P. McCusker, and Judith P. Klinman*

*Department of Chemistry and Department of Molecular and Cell Biology,
University of California, Berkeley, California 94720*

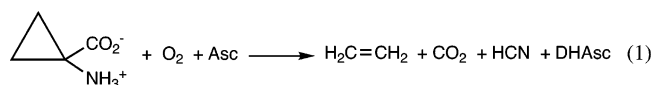*Received June 1, 2006; Revised Manuscript Received August 30, 2006*

ABSTRACT: The behavior of three cyclic and three acyclic analogues of 1-aminocyclopropane-1-carboxylic acid (ACC) with ACC oxidase has been analyzed with regard to turnover rates, product distribution, and O_2 uncoupling. The cyclic analogues all form ethylene, and the acyclic analogues all undergo decarboxylation. The degree of uncoupling varies from almost none (ACC) to 21-fold (glycine), while turnover rates (k_{cat}) are all within a factor of 4-fold of that of ACC. The aggregate data point toward a rate-determining formation of an activated iron−oxo intermediate, which partitions between amine oxidation and reductive uncoupling in a manner that is dependent on substrate structure.

1-Aminocyclopropane 1-carboxylic acid oxidase (ACCO)[1] belongs to the two-histidine, one-carboxylate family of non-heme iron monooxygenases (*1, 2*). The active sites of these enzymes contain a single ferrous ion in an octahedral geometry, which is normally comprised of the 2-histidine, 1-carboxylate facial triad and three water molecules in the resting form of the enzyme. X-ray structures have been determined for a large number of these enzymes, including ACCO (cf. refs *3−6*), indicating an active site that is fairly exposed to solvent and an overall jellyroll motif protein fold that is highly conserved. Despite these similarities, the degree of primary sequence homology is exceptionally low; for example, deacetoxycephalosporin C-synthase and isopenicillin N-synthase share only 19% sequence homology (*3, 5*), with this disparity reflecting, in part, the very different substrate specificities of the member enzymes.

What distinguishes ACCO from the other enzymes of this family is the two-electron donating cosubstrate: ascorbate in the case of ACCO (*7, 8*) and α-ketoglutarate (α-KG) in all other known examples (*2*). A working, consensus mechanism can be developed for the α-ketoglutarate-dependent enzymes, in which binding of substrate and α-KG leads to displacement of the three water molecules; two of the open ligation sites become occupied by the α-KG itself, and the

third site remains open as a site for O_2 attachment (Scheme 1) (*2*). The process of O_2 activation can be visualized as an initial one-electron transfer to O_2 to form a ferric superoxide, followed by decarboxylation of the α-KG to form an activated oxygen intermediate, illustrated as an Fe(IV)−oxo species (Scheme 1). This high-valent oxo species is the presumed "generic" oxidant that carries out the wide range of demonstrated oxidation reactions.

The reaction catalyzed by ACCO is shown in eq 1, indicating the unusual nature of the enzymatic products: ethylene, cyanide, and CO_2 (*7, 8*)

$$\triangle \begin{smallmatrix} CO_2^- \\ NH_3^+ \end{smallmatrix} + O_2 + Asc \longrightarrow H_2C{=}CH_2 + CO_2 + HCN + DHAsc \quad (1)$$

where the two-electron donor is ascorbate (Asc), undergoing oxidation to dehydroascorbate (DHAsc).

From a biological perspective, ACCO occupies a unique niche, being the source of the plant hormone ethylene (*9*). The substrate of ACCO, 1-aminocyclopropane-1-carboxylic acid (ACC), is generated in a preceding step from a pyridoxal phosphate-dependent enzyme, ACC synthase (*10*). Due to the central role of ethylene in fruit ripening, both ACC synthase and ACC oxidase may be suitable targets for regulation of this agriculturally important process (*11*).

Previous studies of ACCO indicated that the binding of O_2 is an ordered process, occurring only after the active site is occupied by ACC; these prior kinetic analyses were unable to distinguish whether the addition of ascorbate preceded or followed that of ACC (*7*). In contrast to the α-KG enzymes, the substrate is believed to complex directly to the iron, with ascorbate occupying an outer sphere-binding pocket (*12*). A second important distinction between ACCO and the α-KG enzymes is that in ACCO both substrate and ascorbate can function as a single electron donor, raising questions regarding the sequence of electron donation to O_2 and the mode of O_2 activation. In this study, we report on the behavior of a series of cyclic and acyclic analogues of ACC with the

---

[1] Abbreviations: BOC, 2-butyloxycarbonyl; DMF, dimethylformaldehyde; TEA, triethylamine; TFA, trifluoroacetic acid; MOPS, 3-(*N*-morpholino)propanesulfonic acid; BSA, bovine serum albumin; AIB, α-aminoisobutyric acid; ACC, 1-aminocyclopropane-1-carboxylic acid; ACC-NH₂, 1-aminocyclopropane 1-carboxamide; N-MeACC, *N*-methyl-1-aminocyclopropane 1-carboxylic acid; ACC-OMe, methyl 1-aminocyclopropane 1-carboxylate; ACCO, ACC oxidase; HPLC, high-performance liquid chromatography; DNPH, dinitrophenylhydrazine; FerroZine, 3-(2-pyridyl)-5,6-diphenyl-1,2,4-triazine-*p,p′*-disulfonic acid, monosodium salt; BLM, bleomycin; YSI, Yellow Springs Instrument; α-KG, α-ketogularate.

Scheme 1:   Proposed Mechanism for Formation of Ferryl−Oxo Species in α-Ketoglutarate-Dependent Enzymes[a]
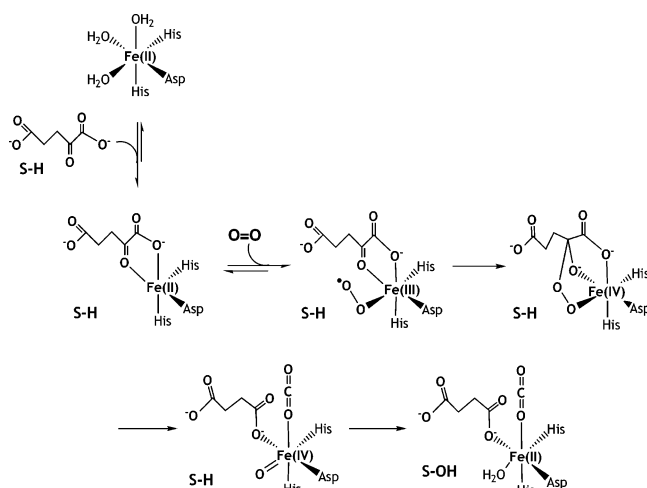
[a] From ref *2*.

goals of defining the relationship between substrate and O_2 activation and the nature of rate-limiting steps in substrate breakdown.

EXPERIMENTAL PROCEDURES

Materials

All reagents were purchased from Sigma or Aldrich unless otherwise indicated. All radiochemicals were purchased from American Radiolabeled Chemicals except for [1-^{14}C]Gly, which was purchased from ICN Biomedicals. The purity of radiolabeled compounds was determined by thin layer chromatography. A known amount of each compound was diluted with a non-radiolabeled standard and spotted on a silica plate. The solvent was an *n*-butanol/acetic acid/water mixture (4:1:1). The compound was localized by staining with either iodine or ninhydrin. Spots were scrapped off into a scintillation vial, and the radioactivity was determined. The purity was determined by measuring the amount of radioactivity that ran with the known non-radiolabeled standard as compared to that of an undeveloped plate. All commercially obtained radiolabeled compounds were >98% pure except [1-^{14}C]ACC, which was ~20% pure.

Synthesis of N-MeACC and N-[methyl-^{14}C]ACC. *N*-Methyl-1-aminocyclopropane 1-carboxylate (N-MeACC) was synthesized as previously described (*13*) with minor modification. The step involving the formation of N-BOC-ACC was carried out overnight at ambient temperature instead of 2 h, resulting in a 98% yield. Anal. Calcd for $C_5H_9NO_2$: 115.06318. Found: 115.06333. N-[*methyl-^{14}C*]ACC was synthesized by the same procedure except for the use of [^{14}C]-CH$_3$I diluted with non-radiolabeled CH$_3$I to a specific activity of 10 μCi/mmol. The purity of N-[*methyl-^{14}C*]ACC was determined by TLC as described above, and was found to be >98%.

Synthesis of the Amide of ACC, ACCNH$_2$. N-BOC-ACC was prepared as described in ref *13* and above. N-BOC-ACC (0.2 g, 1 mmol) and 1-hydroxybenzotriazole hydrate (0.135 g, 1 mmol) were added to anhydrous DMF (5 mL), and the mixture was stirred on ice until the solid dissolved. 1-[3-(Dimethylamino)propyl]-3-ethylcarbodiimide HCl (0.192

g, 1 mmol) was added to the DMF solution and the mixture stirred on ice for 3 h. Anhydrous 7 N NH$_3$ in methanol (1.5 mL, 10 mmol) and TEA (0.3 mL, 2 mmol) were added to the cool mixture, stirred on ice for 1 h, and held overnight at ambient temperature. The DMF was evaporated, and the resulting oil was resuspended in 20 mL of EtOAc and washed with saturated NaHCO$_3$, 0.5 M citric acid, and brine. The organic layer was dried and evaporated to yield a yellow residue. TFA (0.5 mL) was added to the residue, and the mixture was stirred at ambient temperature for 2 h and evaporated. HCl (1 M, 5 mL) was added, and the mixture was stirred briefly and evaporated to yield a yellow oil. Addition of 10 mL of ether precipitated the ACCNH$_2$, which was filtered and dried to yield 134 mg (30%) of white solid.

Methods

Overexpression and Purification of ACCO. ACCO from *Lycopersicon esculentum* (ACO1) was produced in *Escherichia coli* strain BL21(DE3)pLysS and purified by a two-column purification procedure as previously described (*7*).

Initial Velocity Assays. Initial velocities were measured by the rate of oxygen consumption at 25 °C and pH 7.2, using a Yellow Springs Instrument (YSI) biological oxygen monitor (model 5300) as previously described (*7*) with minor modifications. The standard reaction mixture (1 mL) contained 100 mM MOPS (pH 7.2), 20 mM NaHCO$_3$, 100 mM NaCl, 30 mM sodium ascorbate, 0.1 mg/mL BSA, and ACC or substrate analogue at various concentrations. Oxygen concentrations were kept at atmospheric levels and determined using the oxygen monitor that was calibrated with air-saturated water (258 M oxygen at 25 °C). Reactions were initiated with 2 μL of ACCO reconstituted with equimolar Fe(NH$_4$)$_2$(SO$_4$)$_2$. The concentration of ACCO is as indicated in the figure legends. Data from initial velocity experiments with varying substrate concentrations were fitted to the Michaelis−Menten equation using Kaleidagraph.

Ethylene and CO$_2$ Trapping Assays. Standard reaction mixtures were used. For detection of CO$_2$, trace radiolabeled compound was used as appropriate. In both cases, a small dram vial containing the reaction mixture without the enzyme was placed alongside another small vial containing the ethylene or CO$_2$ trap. Both vials were placed in a large vial, which was capped with a septum. The ACCO−Fe(II) complex was introduced into the reaction vial with a syringe, and the contents of both the reaction vial and trap vial were stirred for 1 h. For [^{14}C]CO$_2$ trapping, 1 mL of a solution of freshly prepared 10 M NaOH was used as the trapping agent. At the end of the reaction, the trap was removed and added to 15 mL of scintillation fluid (Hionic-Fluor, Perkin-Elmer) and radioactivity determined by scintillation counting. For ethylene, a 500 μL solution of Br$_2$ in CCl$_4$ was used as the trap. A small amount of 2,5-dibromohexane was added as well, as an internal standard. At the completion of the reaction, a small excess of 2,3-dimethyl-2-butene was added to quench unreacted Br$_2$, and the resulting mixture was analyzed by GC−MS involving a Hewlett-Packard 6890 series gas chromatograph with a 5973 Quadrupole mass spectrometer (using Hewlett-Packard Chemstation). The column was a DB-XLB, 30 m × 250 μm (inside diameter) column, run isothermally at 40 °C and at a flow rate of 10 mL/min. Dibromoethane was purchased from Aldrich for use as the standard.

Table 1: Kinetic Parameters for ACC Oxidase with Various Substrate Analogues[a]

substrate	k_{cat} (min^{-1})	K_m (mM)	substrate	k_{cat} (min^{-1})	K_m (mM)
ACC	36.4 ± 1.4	0.099 ± 0.018			
N-MeACC	12.2 ± 0.5	0.107 ± 0.021	α-AIB	22.1 ± 1.6	0.92 ± 0.29
ACC-NH$_2$	11.3 ± 0.6	0.214 ± 0.047	D-alanine	29.8 ± 0.9	4.42 ± 0.49
ACC-OMe	27.3 ± 1.7	2.76 ± 0.55	glycine	9.5 ± 0.6	1.0 ± 0.4

[a] Kinetic parameters were determined by measuring initial velocities at various concentrations of substrate while maintaining ascorbate and oxygen at a constant concentration: 30 mM ascorbate, 258 μM O$_2$, and 20 mM CO$_2$/bicarbonate.

Product Analysis for Acyclic Substrates. [*methyl*-^{3}H]-α-AIB (50 mM, specific activity of 38 μCi/mmol) or [2,3-^{3}H]-D-Ala (50 mM, specific activity of 20 μCi/mmol) was incubated in the standard reaction mixture described above containing either 20 μM ACCO−Fe(II) complex, 20 μM ACCO−Zn complex and 20 μM Fe(II), or 20 μM BSA and 20 μM Fe(II). Reaction mixtures were incubated open to the atmosphere at ambient temperature for 2 h and reactions quenched with 10 μL of 0.1 M FerroZine to prevent further reaction with free iron. TCA (40%, 50 μL) was added to the reaction mixture, and the solution was stirred for 5 min and centrifuged for 20 min at 14K rpm. The supernatant (200 μL) was analyzed by HPLC using a 250 mm × 4.6 mm Phenomenex Kingsorb 5 μm C18 column (solvent being 0.1% TFA, isocratic for 15 min at room temperature). Fractions were either collected into scintillation vials with the radioactivity determined or collected in Eppendorf tubes for further analysis. Fractions (200 μL) not analyzed by scintillation counting were treated either with 20 μL of 10 mM dinitrophenylhydrazine (DNPH) in a HCl/H$_2$O/CH$_3$CN mixture (2:5:1) or with solvent without DNPH. Reaction mixtures were incubated for 1 h at room temperature. To create an internal standard, ∼250 μmol of acetaldehyde or acetone was added to the reaction mixture and the mixture incubated for an additional 1 h. Reaction mixtures (200 μL) were analyzed by HPLC. The solvent was 0.1% TFA isocratic for 15 min, 0−90% CH$_3$CN with a 0.1% TFA gradient for 15 min, or 90% CH$_3$CN isocratic for 10 min at a flow rate of 1 mL/min. Fractions were collected into scintillation vials, and radioactivity was determined. Absorbance for DNPH derivatives was monitored at 360 nm.

Stoichiometry of O$_2$ Consumption to CO$_2$ Production. Oxygen consumption was assessed using a YSI biological oxygen monitor (model 5300) as described above. Reaction mixtures contained [1-^{14}C]-D-Ala, [1-^{14}C]ACC, [1-^{14}C]-α-AIB, or [1-^{14}C]Gly in trace amounts. Substrates were kept at saturating concentrations (at least 10-fold above K_m), 30 mM ascorbate, and ambient O$_2$ concentrations. Reactions (1 mL) were initiated with a preincubated mixture of ACCO and Fe(II) in a 2:1 ratio. This was done to minimize the amount of free Fe(II) in solution. Final concentrations were typically 10 μM ACCO and 5−6 μM Fe(II). Reactions were quenched by addition of 3 μL of 0.1 M FerroZine, and the O$_2$ consumption rate was allowed to stabilize. The reaction mixture (0.8 mL) was removed with a gastight syringe and injected into a small vial containing 0. 1 mL of 10% HCl that was inside a larger vial containing the CO$_2$ trap (see above). The acidified reaction mixture and the CO$_2$ trap were stirred for 2 h, and radioactivity from [^{14}C]CO$_2$ was determined as described above. Controls measuring the efficiency of the CO$_2$ trap were carried out by injecting a known amount of [^{14}C]NaHCO$_3$ into the vial containing acid,

as described above, and measuring the amount of [^{14}C]CO$_2$ recovered. The efficiency of trapping was routinely ∼98%.

Stoichiometry of O$_2$ Consumption to Ethylene Production. O$_2$ consumption was assessed using an Ocean Optics FOXY fiber optic oxygen sensor. This system was chosen over the YSI model 5300 oxygen electrode since the fiber optic probe can be inserted through a syringe into a septum, making the system completely closed and, thus, preventing the escape of ethylene. Substrates were kept at saturating concentrations (at least 10-fold above K_m), 30 mM ascorbate, and ambient O$_2$ concentrations. The ACCO−Fe(II) complex [final concentrations of 10 μM ACCO and 5 μM Fe(II)] was injected by syringe into a $^1/_2$-dram vial (1.8 mL) covered with a septum with no headspace. The reaction was quenched with FerroZine as described above. A 10 mL syringe filled with air was used to transfer the reaction mixture to a 10 mL test tube covered with a septum using a cannula. The contents of the test tube were stirred vigorously for at least 4 h before ethylene analysis. The amount of ethylene was measured by removing 2 mL of the headspace and injecting this onto a 250 μL loop of a Hewlett-Packard 5890 series gas chromatograph interfaced with a 5973 Quadrupole mass spectrometer. The column, 60 m × 320 μm (inside diameter), was a Chrompack PoraPlotQ column. Ethylene was separated using ultrapure helium (grade 5) as the carrier gas at 40 °C and a flow rate of 1 mL/min, and detection was achieved by flame ionization. Calibration for ethylene was done with Scotty IV mix 3 hydrocarbon standard (Scotty Specialty Gases). The amount of ethylene (in parts per million) was converted to nanomoles of ethylene per unit volume using the ideal gas law. Dilution of ethylene during sampling was taken into account in the calculations.

Density Functional Theory (DFT) Calculations. All calculations were performed using Gaussian 03 (*14*), with the unrestricted B3LYP hybrid functional and a 6-311+G(2d,p) basis set. The geometries of the neutral molecules or radicals were optimized, and each final structure was checked by frequency calculation to be a real minimum without any imaginary frequency. Single-point calculations were performed using the same method, and zero-point and thermal energy corrections were applied to obtain the enthalpies at 298 K and 1 atm in the gas phase. The R$_2$N−H bond dissociation energies (BDEs) were calculated as the enthalpy change for the reaction R$_2$N−H → R$_2$N$^•$ + H$^•$.

RESULTS

Steady-State Kinetics of O$_2$ Consumption with Substrate Analogues. The dependence of the initial velocity of oxygen consumption by the ACCO−Fe(II) complex on the concentration of ACC was compared to that of a series of substrate analogues (Table 1). Either cyclic substrate analogues [N-methyl-ACC (N-MeACC), the amide of ACC (ACC-

NH_2), or the methyl ester of ACC (ACCOMe)] or acyclic substrate analogues [α-aminoisobutyric acid (α-AIB), D-Ala, or Gly] were used. The presence of any one of the substrate analogues resulted in an increase in the rate of O_2 consumption, catalyzed by the ACCO−Fe(II) complex, and, as expected, the dependence of the initial rate on substrate concentration according to Michaelis−Menten kinetics. Ascorbate and oxygen concentrations were kept constant at 30 mM and ~258 μM, respectively. These concentrations were previously shown to be saturating when ACC was the substrate (7) and were assumed to be at saturating concentrations when substrates other than ACC were used. Additionally, measurement of the K_m values for O_2 or ascorbate in the presence of saturating concentrations of N-MeACC resulted in K_m values similar to those when ACC was the substrate (data not shown). This result indicated that perturbations in the substrate structure were not significantly affecting the interaction of O_2 or ascorbate for the enzyme.

The k_{cat} values for the cyclic substrates are at most 3−4-fold slower than that of ACC (Table 1). The K_m values for N-MeACC and $ACCNH_2$ are not significantly altered compared to that of ACC, while K_m for ACCOMe is increased ~28-fold. Spectroscopic studies have identified that both the amine and carboxylate groups of ACC are ligands to active site Fe(II) (8, 12, 15). While it is possible that both N-MeACC and $ACCNH_2$ can form a bidentate ligand to the Fe(II) center, ACCOMe is not capable of such an interaction, a likely contributor to its increased K_m value.

The k_{cat} values for acyclic substrates AIB and D-Ala are very similar to that of ACC, while the k_{cat} for Gly is 4-fold lower (Table 1). Although the amine and carboxylate moieties in the acyclic substrates were not perturbed, the K_m values increased up to 45-fold. This could partially reflect a geometric requirement of the active site for the three-membered ring of ACC (16). Neither D-alaninamide nor glycinamide was a substrate for ACCO.

Bicarbonate or CO_2 has been shown to be a required activator of the ACCO reaction with ACC (8, 17−19). The requirement for and the level of activation by HCO_3^-/CO_2 were determined for the reaction with each substrate analogue. Activity was not detected in any case when HCO_3^-/CO_2 was scrubbed from the assay mixture.

Activity was restored upon addition of HCO_3^- to the assay mixture. The level of activation by HCO_3^-/CO_2 was determined by comparing the initial rates at saturating substrate, ascorbate, and O_2 concentrations in the presence of atmospheric CO_2 [dissolved HCO_3^-, 7.6×10^{-5} M; dissolved CO_2, 1.2×10^{-5} M at pH 7.2 (17)] versus initial rates in the presence of saturating HCO_3^-/CO_2 concentrations (20 mM HCO_3^- added). In each case, when HCO_3^-/CO_2 was at a saturating concentration, there was a 2−4-fold increase in the initial rate as compared to that with atmospheric HCO_3^-/CO_2 concentrations (data not shown). These results indicate that HCO_3^-/CO_2 functions as an activator regardless of the substrate.

Substrate Turnover. Studies of the reaction products are important to the understanding of the chemical mechanism by which ACCO catalyzes its reaction. Previous studies showed that radiolabeled α-AIB was metabolized in mung bean hypocotyls to CO_2 and that this reaction was inhibited by the addition of ACC, suggesting that the (then unidentified) enzyme responsible for ethylene production from ACC

Table 2: Stoichiometry of Oxygen Reduction Catalyzed by ACC Oxidase with Various Substrates

| | ratio of O_2 consumed to product formed | | |
substrate	O_2:CO_2	O_2:ethylene	products detected
ACC	1.18 ± 0.17	1.44 ± 0.22	ethylene, CO_2
N-MeACC	ND[a]	3.17 ± 0.86	ethylene
ACC-NH_2	NA[b]	4.40 ± 1.56	ethylene
ACC-OMe	NA[b]	1.81 ± 0.72	ethylene
α-AIB	1.68 ± 0.12	NA[b]	acetone, CO_2
D-alanine	3.46 ± 0.51	NA[b]	acetaldehyde, CO_2
glycine	21.4 ± 7.9	NA[b]	CO_2

[a] Not determined. [b] Not applicable.

was responsible for α-AIB turnover (20). It was assumed that α-AIB was oxidized at the amino group in a manner similar to that of ACC and degraded to CO_2 and acetone. D-Ala and D-Val were found to be weak inhibitors of ACCO-catalyzed conversion of ACC to ethylene, providing evidence that these two compounds were able to bind to ACCO (21). However, when it was tested as a substrate, no volatile products were reported for the reaction in the presence of D-Ala. Our results show that ACCO consumes O_2 in the presence of either α-AIB or D-Ala at a rate comparable to that with ACC (Table 1). However, this need not be indicative of substrate turnover. There have been several examples of related non-heme iron enzymes that activate O_2 without corresponding substrate turnover in what is called the "uncoupled" reaction (22, 23). In some cases, significant uncoupling occurs even during normal catalysis with the physiological substrate (22) and leads to either reversible or irreversible enzyme inactivation (23, 24). To fully understand the ACCO reaction with the various substrate analogues, it is important in each case to identify the product, if any, and the extent of uncoupling.

The ability of ACCO to turn over ACC or the cyclic substrate analogues (N-MeACC, $ACCNH_2$, or ACCOMe) was determined by the formation of ethylene. Each substrate analogue or ACC was incubated for 1 h with the ACCO−Fe(II) complex in a closed reaction vial containing an ethylene trap that would convert ethylene to dibromoethane (see Experimental Procedures). At the end of the reaction time, the ethylene trap was quenched and analyzed for dibromoethane by GC−MS. Reactions with BSA/Fe(II) were used as a control for nonenzymatic ethylene formation. The formation of ethylene was detected in the reaction vials of ACC and all the cyclic analogues in the presence of the ACCO−Fe(II) complex (Table 2). No ethylene was detected in any of the BSA/Fe(II) reactions. The amount of ethylene formed during the reaction time from the cyclic analogues was lower that from the reaction with ACC (14% for N-MeACC, 13% for $ACCNH_2$, and 79% for ACCOMe, relative to ACC). If the rates of O_2 consumption for the reactions with the different substrates are considered, the k_{cat} for ACCOMe is approximately 75% of that for ACC, which would be consistent with the amount of ethylene produced during the time course of the reaction. However, $ACCNH_2$ and N-MeACC have k_{cat} values ~30% slower than that for ACC but only produced approximately half the predicted ethylene during the reaction time course. Although the purity of both N-MeACC and $ACCNH_2$ by elemental analysis was determined to be >95%, we considered the possibility that a small amount of contaminating ACC could be responsible

for the ethylene formed in these reactions. To determine whether ethylene was being formed from the substrate analogue and not from contaminating ACC, reactions with each analogue were carried out in the presence of increasing concentrations of the ACCO−Fe(II) complex. In the case of a small amount of contamination where the ACC would be quickly depleted during the reaction, the result would be a nonlinear dependence of ethylene production with an increase in ACCO concentration. For ACC and all cyclic analogues, the amount of ethylene production with an increasing concentration of ACCO showed a linear dependence, indicating that ethylene production was due to substrate analogue turnover rather than ACC contamination (data not shown).

Since CO_2 was detected as a product of AIB metabolism in mung bean hypocotyls (*20*), we determined the ability of ACCO to turn over ACC or the acyclic substrate analogues (α-AIB, D-Ala, and Gly) by CO_2 formation. $[1-^{14}C]ACC$, $[1-^{14}C]$-D-Ala, $[1-^{14}C]$-α-AIB, or $[1-^{14}C]Gly$ was incubated with the ACCO−Fe(II) complex in a closed reaction vial containing a CO_2 trap (see Experimental Procedures). The reaction was quenched by acidification, which released any HCO_3^- dissolved in the reaction mixture, allowing contact with the CO_2 trap. The CO_2 trap was then analyzed by scintillation counting for $[^{14}C]CO_2$. As described above, reactions with BSA/Fe(II) provided a control for nonenzymatic breakdown of the substrate. The formation of $[^{14}C]$-CO_2 was detected in the reaction vials of ACC and all the acyclic analogues in the presence of the ACCO−Fe(II) complex, indicating substrate turnover (Table 2). No $[^{14}C]$-CO_2 was detected in the reactions with BSA/Fe(II).

Product Isolation and Identification from Acyclic Substrates. The reactions with α-AIB and D-Ala were further analyzed by incubation of $[methyl-^3H]$-α-AIB or $[2,3-^3H]$-D-Ala with the ACCO−Fe(II) complex, BSA/Fe(II), or ACCO−Zn complex/Fe(II) and separation of the reaction mixture by HPLC (Figure 1A and Table 3 for results with AIB). BSA/Fe(II) was used, as described above, for a control for nonenzymatic substrate breakdown. Since previous literature reported the potential of a second, allosteric iron-binding site on ACCO (*7*), we tested the ability of such a complex to catalyze substrate turnover by using an ACCO−Zn complex with added free Fe(II). ACCO forms a tightly bound stoichiometric complex with Zn, which cannot be displaced by Fe(II) (*7*).

Results from HPLC separation of reactions with $[methyl-^3H]$-α-AIB are shown in Figure 1A and Table 3. Radioactivity clearly eluted in two peaks from the reaction with the ACCO−Fe(II) *methyl* [Figure 1A (■)]. Peak 1 eluted from the column in a position identical to that of the $[methyl-^3H]$-α-AIB standard and was presumed to be substrate. Radioactive material also eluted in two peaks from the reactions with BSA/Fe(II) [Figure 1A (●)] and ACCO−Zn/Fe(II) [Figure 1A (◆)], but in both cases, the amount of radioactivity in peak 2 was much smaller than that from the ACCO−Fe(II) reaction. In the BSA/Fe(II) reaction, almost all of the recovered radioactivity (98.4%) eluted in peak 1 (Table 3). The small amount of radioactivity (1.6%) in peak 2 may represent either some nonenzymatic conversion of AIB to product or, most likely, trailing of radioactive material from peak 1. The total radioactivity recovered from HPLC of the BSA/Fe(II) reaction mixture was as expected according to
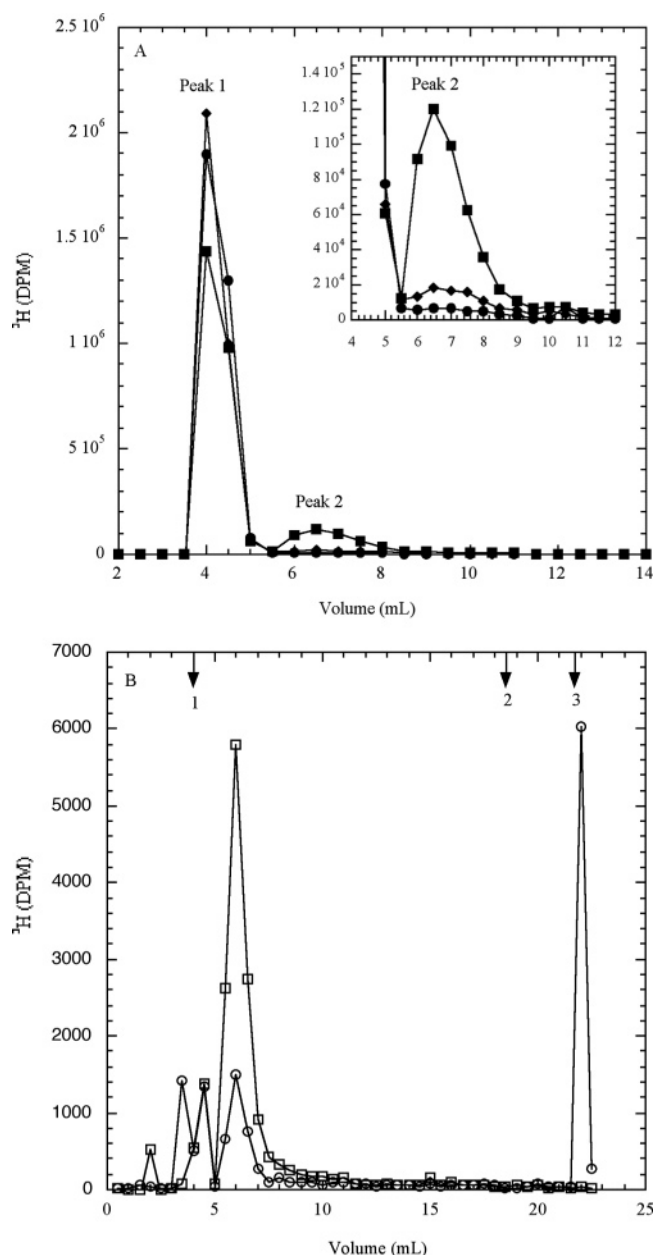

FIGURE 1: HPLC separation and identification of ^3H-labeled product from an ACCO reaction with $[methyl-^3H]$-α-AIB. (A) HPLC separation of ^3H-labeled substrate from ^3H-labeled products: ACCO−Fe(II) (■), ACCO−Zn and Fe(II) (◆), or BSA and Fe(II) (●). (B) DNPH derivatization followed by HPLC analysis. Peak 2 from panel A was treated with (○) or without (□) DNPH and applied to a C18 HPLC column as described in Experimental Procedures. The elution volumes of $[^3H]$-α-AIB (*1*), DNPH (*2*), or acetone treated with DNPH (*3*) are indicated by the numbered arrows. DNPH and the DNPH−acetone derivative were detected by following the absorbance at 355 nm.

the amount of trace $[methyl-^3H]$-α-AIB added, and this value was set to 100% (Table 3). Most of the radioactivity from the ACCO−Zn/Fe(II) reaction eluted in peak 1 (94.9%). However, there was a slight increase in radioactive material eluting in peak 2 (3.4%) compared to that in the BSA/Fe(II) reaction [Figure 1A (◆) and Table 3]. Although the small increase in radioactivity could be due to nonenzymatic reaction by Fe(II) binding to the surface of the ACCO−Zn complex, it more likely represents a slight error in either ACCO concentration or Zn concentration, resulting in a >1:1 ACCO:Zn stoichiometry. At the high concentrations of

Table 3: Recovery of Radioactivity from HPLC Separation of Products from Reaction of ACC Oxidase with [*methyl*-³H]-α-AIB[a]

sample	disintegrations per minute, total	disintegrations per minute, peak 1	disintegrations per minute, peak 2
BSA and Fe(II)	3.33×10^6 (100%)	3.28×10^6 (98.4%)	5.30×10^4 (1.6%)
ACCO−Zn and Fe(II)	3.27×10^6 (98.4%)	3.16×10^6 (94.9%)	1.15×10^5 (3.4%)
ACCO−Fe(II)	2.96×10^6 (89.5%)	2.47×10^6 (74.3%)	4.83×10^5 (14.5%)

[a] Peaks 1 and 2 represent substrate and product, respectively.

ACCO used in the assay, any free ACCO would readily bind to the free Fe(II) in the assay, resulting in active ACCO−Fe(II) complex and a small amount of product formation. Only 90% of the total added radioactivity of the ACCO−Fe(II) reaction was recovered, with 15% of the total added radioactivity in peak 2. The loss of 10% of the total added radioactivity may be due to the volatility of the product, which would have been lost to the atmosphere during the course of the reaction. The results of HPLC analysis for the reaction with [2,3-³H]-D-Ala were similar; i.e., a new radioactive peak was observed in the presence of the ACCO−Fe(II) complex (data not shown). Similar experiments were done with N-[*methyl*-¹⁴C]ACC, but we were unable, with various HPLC columns and conditions, to isolate a product containing the ¹⁴C label from this reaction mixture.

From previous literature, it was predicted that one of the products of α-AIB turnover in mung bean hypocotyls was acetone and that the enzyme responsible for ethylene production was affecting α-AIB turnover (*20*). To further identify if the product from the reaction of ACCO with [*methyl*-³H]-α-AIB was acetone, peak 2 (Figure 1A) was treated with DNPH, which forms derivatives with aldehydes and ketones, and reapplied to the HPLC column. Radioactivity eluting from the HPLC column was monitored, as well as absorbance at 360 nm where both DNPH and the DNPH derivative absorb (Figure 1B). DNPH treatment of peak 2 shifted the elution profile of the radioactive material from 6 mL [Figure 1B (□)] to a new peak eluting at 22 mL [Figure 1B (○)]. Furthermore, the new peak had an absorbance at 360 nm, characteristic of a DNPH derivative, and eluted at a position identical to that of the DNPH derivative of acetone. DNPH alone, as monitored by absorbance, eluted from the column in 18.5 mL. DNPH treatment of [*methyl*-³H]-α-AIB did not result in an altered elution profile, indicating DNPH did not react with AIB (data not shown). The corresponding peak 2 from the reaction of the ACCO−Fe(II) complex with [2,3-³H]-D-Ala was analyzed in an identical way. The product was identified as acetaldehyde (data not shown).

Stoichiometry of O₂ Consumed to Product Formed. Our results suggest that ACCO is capable of processing a wide variety of small amino acid-like substrates. The ability of the enzyme to couple O₂ activation with substrate activation is critical to preventing deleterious reactive oxygen species from being formed and reacting with and potentially inactivating the enzyme. Previous studies with native apple ACCO showed that for every 1.2 O₂ molecules consumed only one molecule of ethylene is produced from the reaction with ACC (*17*). ACCO is known to undergo inactivation under catalytic conditions by an unknown mechanism (*24*), and it is likely that the slightly higher ratio of O₂ consumed to product formed reflects a small amount of uncoupling by the enzyme during catalysis.

The extent of uncoupling for ACCO with both cyclic and acyclic substrate analogues was determined by comparing

the amount of O₂ consumed and product (either ethylene or CO₂) formed. All reactions were carried out at saturating substrate and ascorbate concentrations to minimize the potential O₂ reaction in the absence of substrate. Enzyme was reconstituted with 0.6 equiv of Fe(II) and kept at a high concentration (12-fold higher than the K_d of 0.5 μM) to minimize the amount of free Fe(II) in the reaction mixture. O₂ measurements were taken during or just as the linear phase of the reaction began to fall off due to either loss of Fe(II) from the enzyme or possible enzyme inactivation. A caveat to these measurements is that there is always a background loss of O₂ due to reaction with ascorbate and/or Fe(II) in solution. Although measures were taken to minimize changes in the background O₂ consumption rate before, during, and after the reaction (see above and Experimental Procedures), there is no practical way to completely ensure the background rate is constant during the analysis. Therefore, the data tend to have fairly high standard deviations. However, our results are sufficiently accurate to be able to distinguish between extreme cases of uncoupling.

For cyclic substrate analogues and ACC, the stoichiometry was determined by comparing O₂ consumption with ethylene formation by GC-FID. For the acyclic substrate analogues that were shown to release CO₂ as a product, as well as ACC, O₂ consumption was compared with the formation of [¹⁴C]-CO₂. Ratios of O₂ consumption to product formation are listed in Table 2. The stoichiometry of O₂ consumed to ethylene produced for ACC is 1.44 and to CO₂ produced is 1.18, which is similar to that reported by Dong et al. (*17*). It is uncertain why the ratio of O₂ to ethylene is higher, although within error, than that of O₂ to CO₂. It is unlikely that this reflects a difference in the amount of ethylene versus CO₂ produced. Rather, it is probably due to the extreme volatility of ethylene. The experimental method requires transfer of the reaction solution containing dissolved ethylene from a closed vial to a tube for GC-FID analysis. This method could potentially result in the escape of small amounts of ethylene, therefore making the ratio of O₂ to ethylene appear larger.

All cyclic and acyclic substrates exhibited some increased level of uncoupling over ACC. However, with the cyclic substrates there was no correlation between the extent of uncoupling and whether the amine (MeACC) or the carboxylate (ACCNH₂ or ACCOMe) functional group had been perturbed. In the case of the acyclic substrates, a more definite pattern in which the extent of uncoupling was affected by the substrate structure emerged. Breaking the cyclic ring but keeping both methyl groups in α-AIB resulted in some increased level of uncoupling over the ACC reaction (1.7 O₂:CO₂ ratio for AIB versus 1.2 for ACC). However, each successive removal of a methyl group from AIB to Ala and then to Gly resulted in a further increase in the extent of uncoupling, with Gly having the most extreme effect of

Table 4: N−H Homolytic BDEs for Substrates of ACC Oxidase

compound	BDE (kcal/mol)	compound	BDE (kcal/mol)
ACC	97.4	α-AIB	100.0
N-MeACC	91.4	D-alanine	98.8
ACC-NH$_2$	87.1	glycine	99.0
ACC-OMe	97.3		

only one of every ~21 reactions with O$_2$ resulting in CO$_2$ production.

Calculation of Bond Dissociation Energies for the Amines. As a frame of reference for the interpretation of the rates and product ratios among the amines studied herein, DFT calculations were performed to obtain the bond dissociation energies for removal of a hydrogen atom from the amine functional group. These are summarized in Table 4. The validity of the theoretical method was tested by calculating the N−H BDEs in ammonia, methylamine, and dimethylamine, which provided values that were in good agreement with the experimental data (*25*). The calculated values for the different substrates show that there is not a significant variation in BDEs, except in the case of N-MeACC and ACC-NH$_2$, which have weaker N−H bonds. This suggests that there is no correlation between N−H BDE and the k_{cat} values of these substrates, since N-MeACC and ACC-NH$_2$ do not exhibit dramatically increased rates for the enzymatic reaction.

DISCUSSION

The enzymatic production of ethylene from ACC proceeds by binding of ascorbate, ACC, and O$_2$ to the enzyme to form a ternary complex (*7, 26*). Activation of ACC is likely to occur by abstraction of one electron or a hydrogen atom from the amine by a yet unknown iron−oxo species to form an aminyl radical cation or amine radical, respectively. Rapid radical rearrangement results in cleavage of the cyclopropane ring and eventually formation of ethylene, HCN, and CO$_2$ (*16*). In this study, we demonstrate that ACCO is capable not only of O$_2$ uptake in the presence of various cyclic and acyclic ACC analogues but also of product formation. We have also determined the extent that O$_2$ activation is coupled to product formation from each of these analogues.

Proposal of Rate-Limiting Formation of the Fe(IV)=O Intermediate Prior to Substrate Activation. Scheme 2 summarizes our proposed mechanism of the ACCO reaction for cyclic and acyclic substrates up through substrate activation and the first step committing the enzyme to product formation. We have depicted the Fe(IV)=O intermediate (Scheme 2, **3**) as the species directly responsible for the first step in substrate activation, namely the one-electron oxidation of the amine to form the amine radical (Scheme 2, **4**). As shown in Scheme 1, the Fe(IV)=O intermediate has been implicated as the species that activates substrate in the α-ketoglutarate-dependent enzymes (*27*), where formation of this species is linked to the two-electron oxidative decarboxylation of α-ketoglutarate in these enzymes. However, ACCO uses ascorbate rather than α-ketoglutarate as the reductant, which, unlike the decarboxylation of α-ketoglutarate, can donate either one or two electrons. Thus, there is the potential for the formation of two iron−oxo species that could be responsible for substrate activation in ACCO: Fe(III)−OOH and Fe(IV)=O (**2** and **3**, respectively, in Scheme 2).

Although both iron−oxo species have been suggested to activate substrate (*8*), neither species has been observed, thus far. In the event that semidehydroascorbate remains bound to the enzyme, we would expect this species to outcompete the substrate in the reductive cleavage of the peroxy bond to yield the high-valent Fe(IV)=O intermediate.

Importantly, the data summarized in Table 1 demonstrate that k_{cat} is almost insensitive to substrate structure among a series of acyclic and cyclic substrates. As discussed below, the cyclic and acyclic substrates follow diverging chemical pathways to form different products with rates that may vary by 100-fold. The finding that k_{cat} is almost unchanged by substrate and, by extension, product structures, together with the difference in BDEs for ACC-NH$_2$ and N-MeACC versus the other amines (Table 4), points toward a rate-limiting step that precedes substrate activation. In single-turnover experiments (*8*), it has been proposed that reduction of Fe(III) to Fe(II) may limit enzyme cycling. On the basis of driving force considerations (*28*) and the very high concentration of ascorbate used herein (30 mM), we consider this unlikely in this study. We therefore propose the rate-determining step involves reaction between ascorbate and Fe(III)(O$_2$$^{•-}$) to yield oxidized ascorbate and an activated iron−oxo intermediate as the species responsible for all subsequent chemistry (Scheme 2).

Chemical Mechanism for Acyclic Substrate Breakdown. Identification of the products of acyclic substrate oxidation by ACCO allows us to postulate a chemical mechanism that is based on previous literature of model compounds. It is likely and expected that acyclic substrate activation begins with either a one-electron oxidation or hydrogen atom abstraction (*16*) in forming the amine radical (Scheme 2). However, fragmentation of the iron-complexed amine radical cation by a C−C bond cleavage analogous to ACC ring opening would result in the corresponding imine and a formate radical. Another pathway for the origin of the C−C bond cleavage reaction in acyclic substrates is decarboxylation, which would lead to a carbanion that is stabilized by its interaction with the metal-complexed radical center on the adjacent amine. A second one-electron oxidation step would lead to the corresponding imine, which can be hydrolyzed to yield the aldehyde or ketone product and ammonia.

Support for radical-based decarboxylation comes from experiments in which the decay of α-aminocarboxylate aminium radical cations in solution is examined. Su et al. (*29*) showed that decay occurred predominantly by decarboxylation to form a carbon radical intermediate with a rate of approximately 10^6 s^{-1}. Measurement of the α-CH acidities demonstrated that the proximity of a positively charge heteroatom greatly altered the extent of carbon radical intermediate formation. The pK_a of α-C dropped by ~20 pK_a units (to ~10) when the carbon atom was adjacent to an amine radical cation compared to a deprotonated amine [pK_a ~ 30 (*30*)].

These considerations provide support for the proposal that the rate-determining step in the ACCO reaction precedes substrate activation. As summarized in Scheme 2, and discussed above, rates of decarboxylation of model compounds have been determined to be ~10^6 s^{-1} (*29*), whereas the rate of cyclopropane ring opening is estimated to be ~10^8 s^{-1} (*31*), a 100-fold difference that is not reflected in the

Scheme 2: Proposed Mechanism for Oxidation of Cyclic and Acyclic Substrates by ACCO, Illustrated with ACC and α-AIB
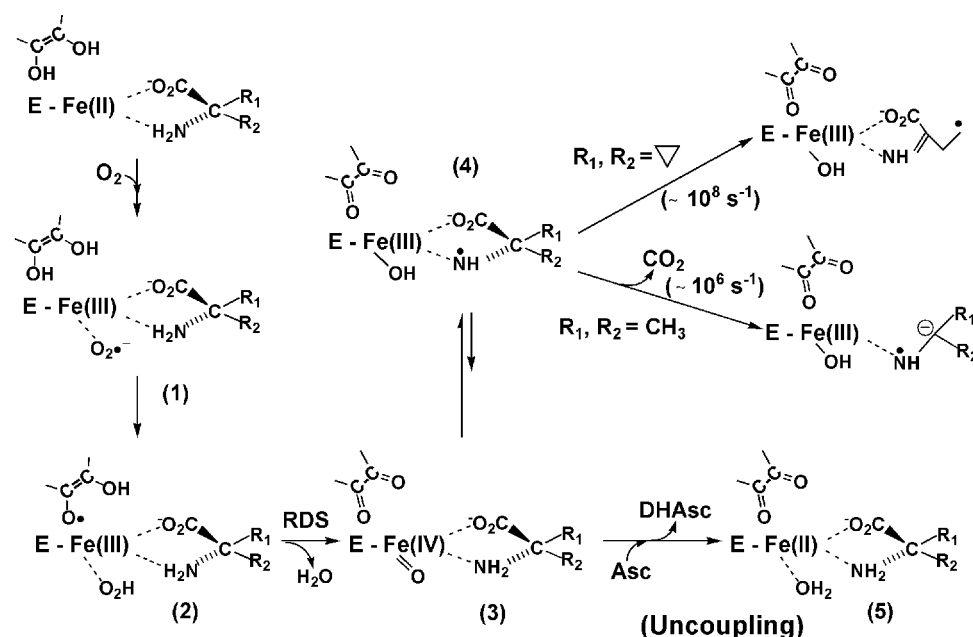
observed k_{cat} values. This argues that neither ring opening from the cyclic substrates nor loss of CO_2 from the acyclic substrates is the controlling step in the mechanism. Though it is often observed that a common step such as product release limits an enzymatic process, this also appears to be incompatible with the data presented here, since the various ACCO substrate analogues are forming different products that may be expected to dissociate at different rates. Finally, it seems unlikely that the initial oxidation of amine substrates is rate-determining, since this would also be expected to be influenced by substrate structure (Table 4), in contrast to the experimental observations (Table 1). Rather, as described below, variations in substrate structure appear to be affecting the ratio of amine oxidation to oxidative uncoupling.

Branching between O_2 Uncoupling and Substrate Activation. As summarized in Table 2, stoichiometry experiments have been carried out that allow a comparison of the amount of O_2 consumed to the amount of product formed. Results show that perturbation of the substrate structure does indeed cause an increase in the yield of the uncoupled reaction. Although no direct correlation could be detected between uncoupling and manipulation of the cyclic substrates at the amine or carboxylate functional groups, the uncoupling in the presence of the acyclic substrates shows a pattern in which loss of methyl groups on α-C increases the level of uncoupling. Scheme 2 therefore includes a branch point in which O_2 activation becomes uncoupled from substrate activation. This is proposed to occur when reaction of the putative oxygen-activated intermediate [Fe(IV)=O] with excess ascorbate becomes competitive with substrate oxidation, leading to the four-electron-reduced H_2O as the product and the active Fe(II) form of the enzyme (**5** in Scheme 2). For all substrates, coupling is expected to be governed by the ability of the substrate to be properly positioned for oxidation. Once the aminyl radical has been formed, the large driving force for decarboxylation, and even larger driving force for ring opening, will commit the respective chemical intermediate to product formation. Uncoupling occurs when the rate of substrate oxidation is decreased enough that the

rate of reaction with ascorbate becomes a competing reaction. In the case of N-MeACC and ACC-NH$_2$, we expected that the rate of amine oxidation would, in fact, be increased compared to that of ACC, based on the calculated BDEs (cf. Table 4). However, our results indicate that this is not the case and that the rate of substrate activation is decreased such that the uncoupled reaction predominates. It is likely that the presence of the methyl group causes steric hindrance and that N-MeACC is incapable of the correct binding orientation for its reaction with the activated oxygen center to occur efficiently. Such a model is also likely in the case of ACCNH$_2$, where one of the iron ligands has been modified from a negatively charged carboxylate to a neutral amide. It is currently unclear whether ACCNH$_2$ and ACCOMe are even capable of the bidentate binding to the iron center that is characteristic of ACC. We note that in the case of the acyclic substrates the pattern of an increased level of uncoupling with a decreasing number of substituents at the α-carbon could, in principle, reflect the rate of decarboxylation since the stability of the resulting carbon radical intermediate is expected to be influenced by the degree of substitution:
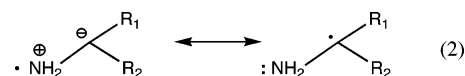
However, the anticipated rapid loss of CO_2 from the metal-complexed oxidized acyclic substrate makes it unlikely that such carbon radical stability controls the degree of uncoupling. Noting the trends in uncoupling with the alternate cyclic substrates, together with the large K_m values for acyclic substrates in relation to ACC, we conclude that a more likely explanation is a role for R_1 and R_2 in aligning substrate near the active site iron center such that the initial oxidation at the amine functional group can occur.

In conclusion, the cyclic and acyclic analogues studied herein offer insight into the nature of rate-limiting steps and reactive chemical intermediates in ACCO and provide a working mechanistic model for ongoing studies. Future

experiments will focus on efforts to monitor the formation of activated iron−oxo species and to isolate the remaining products from the reaction with the cyclic analogues. The latter should provide information about the nature of the cryptic intermediates that lie between the substrate radical and the final products.

REFERENCES

1. Schofield, C. J., and Zhang, Z. H. (1999) Structural and mechanistic studies on 2-oxoglutarate-dependent oxygenases and related enzymes, *Curr. Opin. Struct. Biol. 9*, 722−731.
2. Costas, M., Mehn, M. P., Jensen, M. P., and Que, L., Jr. (2004) Dioxygen activation at mononuclear nonheme iron active sites: Enzymes, models, and intermediates, *Chem. Rev. 104*, 939−986.
3. Roach, P. L., Clifton, I. J., Fulop, V., Harlos, K., Barton, G. J., Hajdu, J., Andersson, I., Schofield, C. J., and Baldwin, J. E. (1995) Crystal-Structure of Isopenicillin N-Synthase Is the First from a New Structural Family of Enzymes, *Nature 375*, 700−704.
4. Zhang, Z. H., Ren, J. S., Harlos, K., Mckinnon, C. H., Clifton, I. J., and Schofield, C. J. (2002) Crystal structure of a clavaminate synthase-Fe(II)-2-oxoglutarate-substrate-NO complex: Evidence for metal centred rearrangements, *FEBS Lett. 517*, 7−12.
5. Valegård, K., Van Scheltinga, A. C. T., Lloyd, M. D., Hara, T., Ramaswamy, S., Perrakis, A., Thompson, A., Lee, H. J., Baldwin, J. E., Schofield, C. J., Hajdu, J., and Andersson, I. (1998) Structure of a cephalosporin synthase, *Nature 394*, 805−809.
6. Zhang, Z. H., Ren, J. S., Clifton, I. J., and Schofield, C. J. (2004) Crystal structure and mechanistic implications of 1-aminocyclopropane-1-carboxylic acid oxidase: The ethylene-forming enzyme, *Chem. Biol. 11*, 1383−1394.
7. Thrower, J. S., Blalock, R., and Klinman, J. P. (2001) Steady-state kinetics of substrate binding and iron release in tomato ACC oxidase, *Biochemistry 40*, 9717−9724.
8. Rocklin, A. M., Kato, K., Liu, H. W., Que, L., Jr., and Lipscomb, J. D. (2004) Mechanistic studies of 1-aminocyclopropane-1-carboxylic acid oxidase: Single turnover reaction, *J. Biol. Inorg. Chem. 9*, 171−182.
9. John, P. (1997) Ethylene biosynthesis: The role of 1-aminocyclopropane-1-carboxylate (ACC) oxidase, and its possible evolutionary origin, *Physiol. Plant. 100*, 583−592.
10. Capitani, G., Hohenester, E., Feng, L., Storici, P., Kirsch, J. F., and Jansonius, J. N. (1999) Structure of 1-aminocyclopropane-1-carboxylate synthase, a key enzyme in the biosynthesis of the plant hormone ethylene, *J. Mol. Biol. 294*, 745−756.
11. Hamilton, A. J., Lycett, G. W., and Grierson, D. (1990) Antisense Gene That Inhibits Synthesis of the Hormone Ethylene in Transgenic Plants, *Nature 346*, 284−287.
12. Zhou, J., Rocklin, A. M., Lipscomb, J. D., Que, L., Jr., and Solomon, E. I. (2002) Spectroscopic studies of 1-aminocyclopropane-1-carboxylic acid oxidase: Molecular mechanism and CO_2 activation in the biosynthesis of ethylene, *J. Am. Chem. Soc. 124*, 4602−4609.
13. Vaidyanathan, G., and Wilson, J. W. (1989) Reaction of Cyclopropanamines with Hypochlorite, *J. Org. Chem. 54*, 1815−1820.
14. Frisch, M. J., Trucks, G. W., Schlegel, H. B., Scuseria, G. E., Robb, M. A., Cheeseman, J. R., Montgomery, J. A., Jr., Vreven, T., Kudin, K. N., Burant, J. C., Millam, J. M., Iyengar, S. S., Tomasi, J., Barone, V., Mennucci, B., Cossi, M., Scalmani, G., Rega, N., Petersson, G. A., Nakatsuji, H., Hada, M., Ehara, M., Toyota, K., Fukuda, R., Hasegawa, J., Ishida, M., Nakajima, T., Honda, Y., Kitao, O., Nakai, H., Klene, M., Li, X., Knox, J. E., Hratchian, H. P., Cross, J. B., Bakken, V., Adamo, C., Jaramillo, J., Gomperts, R., Stratmann, R. E., Yazyev, O., Austin, A. J., Cammi, R., Pomelli, C., Ochterski, J. W., Ayala, P. Y., Morokuma, K., Voth, G. A., Salvador, P., Dannenberg, J. J., Zakrzewski, V. G., Dapprich, S., Daniels, A. D., Strain, M. C., Farkas, O., Malick,
D. K., Rabuck, A. D., Raghavachari, K., Foresman, J. B., Ortiz, J. V., Cui, Q., Baboul, A. G., Clifford, S., Cioslowski, J., Stefanov, B. B., Liu, G., Liashenko, A., Piskorz, P., Komaromi, I., Martin, R. L., Fox, D. J., Keith, T., Al-Laham, M. A., Peng, C. Y., Nanayakkara, A., Challacombe, M., Gill, P. M. W., Johnson, B., Chen, W., Wong, M. W., Gonzalez, C., and Pople, J. A. (2003) *Gaussian 03*, Gaussian, Inc., Pittsburgh, PA.
15. Rocklin, A. M., Tierney, D. L., Kofman, V., Brunhuber, N. M. W., Hoffman, B. M., Christoffersen, R. E., Reich, N. O., Lipscomb, J. D., and Que, L., Jr. (1999) Role of the nonheme Fe(II) center in the biosynthesis of the plant hormone ethylene, *Proc. Natl. Acad. Sci. U.S.A. 96*, 7905−7909.
16. Pirrung, M. C. (1999) Ethylene biosynthesis from 1-aminocyclopropanecarboxylic acid, *Acc. Chem. Res. 32*, 711−718.
17. Dong, J. G., Fernández-Maculet, J. C., and Yang, S. F. (1992) Purification and Characterization of 1-Aminocyclopropane-1-Carboxylate Oxidase from Apple Fruit, *Proc. Natl. Acad. Sci. U.S.A. 89*, 9789−9793.
18. Fernández-Maculet, J. C., Dong, J. G., and Yang, S. F. (1993) Activation of 1-Aminocyclopropane-1-Carboxylate Oxidase by Carbon Dioxide, *Biochem. Biophys. Res. Commun. 193*, 1168−1173.
19. Zhang, Z. H., Schofield, C. J., Baldwin, J. E., Thomas, P., and John, P. (1995) Expression, purification and characterization of 1-aminocyclopropane-1-carboxylate oxidase from tomato in *Escherichia coli*, *Biochem. J. 307*, 77−85.
20. Liu, Y., Su, L. Y., and Yang, S. F. (1984) Metabolism of α-Aminoisobutyric-Acid in Mungbean Hypocotyls in Relation to Metabolism of 1-Aminocyclopropane-1-carboxylic Acid, *Planta 161*, 439−443.
21. Gibson, E. J., Zhang, Z. H., Baldwin, J. E., and Schofield, C. J. (1998) Substrate analogues and inhibition of ACC oxidase: Conversion of D-valine to iso-butanal, *Phytochemistry 48*, 619−624.
22. Holme, E., Lindstedt, S., and Nordin, I. (1982) Uncoupling in the γ-Butyrobetaine Hydroxylase Reaction by D-Carnitine and L-Carnitine, *Biochem. Biophys. Res. Commun. 107*, 518−524.
23. Liu, A., Ho, R. Y. N., and Que, L. (2001) Alternative reactivity of an α-ketoglutarate-dependent Iron(II) oxygenase: Enzyme self-hydroxylation, *J. Am. Chem. Soc. 123*, 5126−5127.
24. Barlow, J. N., Zhang, Z. H., John, P., Baldwin, J. E., and Schofield, C. J. (1997) Inactivation of 1-aminocyclopropane-1-carboxylate oxidase involves oxidative modifications, *Biochemistry 36*, 3563−3569.
25. Gomes, J. R. B., Da Silva, M., and Da Silva, M. (2004) Solvent and structural effects in the N-H bond homolytic dissociation energy, *J. Phys. Chem. A 108*, 2119−2130.
26. Brunhuber, N. M. W., Mort, J. L., Christoffersen, R. E., and Reich, N. O. (2000) Steady-state kinetic mechanism of recombinant avocado ACC oxidase: Initial velocity and inhibitor studies, *Biochemistry 39*, 10730−10738.
27. Price, J. C., Barr, E. W., Tirupati, B., Bollinger, J. M., and Krebs, C. (2003) The first direct characterization of a high-valent iron intermediate in the reaction of an α-ketoglutarate-dependent dioxygenase: A high-spin Fe(IV) complex in taurine/α-ketoglutarate dioxygenase (TauD) from *Escherichia coli*, *Biochemistry 42*, 7497−7508.
28. Although the Fe(III)/Fe(II) redox potential in ACCO has not been determined, the redox potential for dehydroascorbate (A$^{•−}$)/ ascorbate (HA$^−$) is ca. 0.3 V [Williams, N. H., and Tandell, J. K. (1982) Outer sphere electron transfer reactions of ascorbate anion, *Aust. J. Chem. 35*, 1133−1144]. The redox potential for Fe(III)/ Fe(II) is highly dependent on whether the metal is free (0.77 V) or protein-bound [note that this potential varies from ca. 0.1 to 0.4 V for Fe(III) bound to the heme of various cytochromes] [Loach, P. A. (1976) Physical and Chemical Data, in *Handbook*

of Biochemistry and Molecular Biology (Fasman, G. D., Ed.) 3rd ed., Vol. 1, pp 122−130, CRC Press, Boca Raton, FL].

29. Su, Z. Y., Falvey, D. E., Yoon, U. C., and Mariano, P. S. (1997) The dynamics of α-anilino carboxylate and related cation radical α-heterolytic fragmentations, *J. Am. Chem. Soc. 119*, 5261−5262.

30. Zhang, X. M., Yeh, S. R., Hong, S., Freccero, M., Albini, A., Falvey, D. E., and Mariano, P. S. (1994) Dynamics of α-CH Deprotonation and α-Desilylation Reactions of Tertiary Amine Cation Radicals, *J. Am. Chem. Soc. 116*, 4211−4220.

31. Griller, D., and Ingold, K. U. (1980) Free-Radical Clocks, *Acc. Chem. Res. 13*, 317−323.